Eur. J. Biochem. **270**, 1474–1482 (2003) © FEBS 2003 doi:10.1046/j.1432-1033.2003.03513.x

Kinetic mechanisms of glycine oxidase from *Bacillus subtilis*

Gianluca Molla, Laura Motteran, Viviana Job, Mirella S. Pilone and Loredano Pollegioni

Department of Structural and Functional Biology, University of Insubria, Varese, Italy

The kinetic properties of glycine oxidase from *Bacillus subtilis* were investigated using glycine, sarcosine, and D-proline as substrate. The turnover numbers at saturating substrate and oxygen concentrations were 4.0 s^{-1}, 4.2 s^{-1}, and 3.5 s^{-1}, respectively, with glycine, sarcosine, and D-proline as substrate. Glycine oxidase was converted to a two-electron reduced form upon anaerobic reduction with the individual substrates and its reductive half-reaction was demonstrated to be reversible. The rates of flavin reduction extrapolated to saturating substrate concentration, and under anaerobic conditions, were 166 s^{-1}, 170 s^{-1}, and 26 s^{-1}, respectively, with glycine, sarcosine, and D-proline as substrate. The rate of reoxidation of reduced glycine oxidase with oxygen in the absence of product (extrapolated rate $\approx 3 \times 10^4$ $M^{-1} \cdot s^{-1}$) was too slow to account for catalysis and thus reoxidation started from the reduced enzyme:imino acid complex. The kinetic data are compatible with a ternary complex sequential mechanism in which the rate of product dissociation from the reoxidized enzyme form represents the rate-limiting step. Although glycine oxidase and D-amino acid oxidase differ in substrate specificity and amino acid sequence, the kinetic mechanism of glycine oxidase is similar to that determined for mammalian D-amino acid oxidase on neutral D-amino acids, further supporting a close similarity between these two amine oxidases.

Keywords: amine oxidase; glycine oxidase; flavoenzyme; kinetic mechanism; reaction mechanism.

Glycine oxidase is the product of the *yjb*R gene of *Bacillus subtilis* that was predicted by sequence homology to be a flavoprotein similar to sarcosine oxidase [1,2]. Three previous investigations reported on the cloning and production of the glycine oxidase gene in *Escherichia coli* (the recombinant enzyme produced was up to 3.9% of total soluble proteins in crude extract) and on the protein purification and characterization [2–4]. The protein is a homotetrameric flavoenzyme containing 1 mol of noncovalently bound FAD per 47 kDa protein monomer. Glycine oxidase catalyzes the oxidative deamination of various primary and secondary amino acids (e.g. sarcosine, *N*-ethylglycine, and glycine) and D-amino acids (e.g. D-alanine, D-proline, D-valine, etc.) to form the corresponding α-keto acids and hydrogen peroxide. Glycine oxidase seems to partially share substrate specificity with various flavooxidases, such as D-amino acid oxidase (DAAO, EC 1.4.3.3) and sarcosine oxidase (SOX, EC 1.5.3.1), and also appears to be stereospecific in the oxidation of the D-isomer of the amino acids tested [3,4].

D-Amino acid oxidase (containing 1 mol of noncovalently bound FAD per 40 kDa monomer) catalyzes the oxidative deamination of neutral and (less efficiently) basic D-amino acids to give the corresponding α-keto acids, ammonia, and hydrogen peroxide [5,6]. Acidic D-amino acids are oxidized by D-aspartate oxidase, and D-proline is the only D-amino acid oxidized by both D-amino acid oxidase and D-aspartate oxidase. On the other hand, SOX catalyzes the oxidative demethylation of sarcosine to yield glycine, hydrogen peroxide, and formaldehyde [7]. The sarcosine oxidases can be subdivided into two different classes: heterotetrameric (TSOX) and monomeric (MSOX) enzymes. Only TSOX uses tetrahydrofolate as substrate. The heterotetrameric SOXs are composed of four different subunits (from 10 to 100 kDa) and also contain noncovalently bound FAD, noncovalently bound NAD^+, and covalently bound FMN, which is linked to the β-subunit (42–45 kDa). The monomeric SOXs are similar in size to the β-subunit of TSOX and contain covalently bound FAD.

In a previous paper, we demonstrated that glycine oxidase can be distinguished from SOX as it catalyzes the deamination of amino acids, shows a high pK_a for flavin N(3)H ionization, does not bind covalently the FAD cofactor, and reacts readily with sulfite. In all these properties glycine oxidase resembles D-amino acid oxidase [3]. On the other hand, D-amino acid oxidase does not oxidize sarcosine, and glycine is a poor substrate (the turnover number on this substrate is less than 1% of the activity on D-alanine) [5]. According to investigations of the substrate specificity and of the binding properties, the glycine oxidase active site seems to preferentially accommodate amines of small size such as glycine and sarcosine. In fact, glycolate, a compound similar to the substrate

Correspondence to L. Pollegioni, Department of Structural and Functional Biology, University of Insubria, via J. H. Dunant 3, 21100 Varese, Italy.
Fax: + 39 0332 421500, Tel.: + 39 0332 421506,
E-mail: loredano.pollegioni@uninsubria.it

Abbreviations: EMTN, enzyme monitored turnover; E-FAD_{ox}, oxidized form of the enzyme; E-FAD_{red}, reduced form of the enzyme; IA, imino acid; MSOX, monomeric sarcosine oxidase; TSOX, heterotetrameric sarcosine oxidase.

Enzymes: glycine oxidase (GO, EC 1.4.3.19); D-amino acid oxidase (DAAO, EC 1.4.3.3); sarcosine oxidase (SOX, EC 1.5.3.1); horseradish peroxidase (HRP, EC 1.11.1.7).

Note: a web site is available at http://dipbsf.uninsubria.it/dbsf/

(Received 8 January 2003, revised 5 February 2003, accepted 10 February 2003)

glycine, was demonstrated to bind glycine oxidase the tightest (K_d = 0.6 mM) and to act as a competitive inhibitor with respect to sarcosine. The high apparent K_m value determined for D-alanine and the inability to bind dimethylglycine indicates that glycine oxidase binding to compounds with a central carbon atom with a sp3 hybridization or with three substituents larger than an H atom is hindered by steric hindrance. The presence of a carboxylic group and an amino group is not mandatory for binding and catalysis. Furthermore, the analysis of the binding data for glycine oxidase and linear aliphatic acids suggests that each methylene group contributes very little to binding energy (0.8–1.7 kJ·mol^{-1}) [4]. The overall binding properties of glycine oxidase profoundly distinguish it from D-amino acid oxidase.

In the present study we investigated the kinetic properties of *B. subtilis* glycine oxidase using three different substrates (namely, glycine, sarcosine, and D-proline). Comparing these properties with the 3D structures of the corresponding oxidases [8–10], particularly in light of the data presented here, will considerably expand our understanding of the evolution and the mode of functioning of this class of enzymes. The main goal of this project was to elucidate the structure-function relationships in glycine oxidase, with the aim of clarifying the modulation of the substrate specificity in enzymes active on similar compounds.

Materials and methods

Reagents and enzymes

Glycine oxidase was produced and purified from recombinant BL21(DE3)pLysS *E. coli* cells carrying the pT7-HisGO expression plasmid as reported by Job *et al.* [3]. The recombinant enzyme used in these experiments contains an N-terminal His-tag sequence. All other reagents were of the highest purity commercially available.

Absorption measurements

UV-visible absorption spectra were recorded with a Uvikon 930 spectrophotometer (Kontron Instr.) in disodium pyrophosphate buffer, pH 8.5, at 25 °C. Enzyme concentration was determined in terms of flavin content using an ε_{455nm} = 11800 M^{-1}·cm^{-1} [4]. The product composition of the reaction of glycine oxidase with D-proline as substrate was analyzed as outlined by Job *et al.* [4].

Rapid reaction (stopped-flow) measurements

Rapid reaction measurements and turnover experiments were carried out at 25 °C in 75 mM disodium pyrophosphate buffer, pH 8.5, in a BioLogic SFM-300 stopped-flow spectrophotometer equipped with a thermostat and a J & M diode array detector. All concentrations mentioned in these experiments refer to those after mixing. Rapid reactions were routinely recorded in the 200- to 700-nm wavelength range using a scan time of 1 ms per spectrum. For reductive half-reaction experiments, enzyme solutions were made anaerobic in tonometers by 10 cycles of evacuation and equilibration with oxygen-purged argon, and substrate solutions were made anaerobic by bubbling with argon for at least 10 min in glass syringes [11]. The substrate concentration was varied over a sufficient range to obtain information about both the saturation of observed rates and K_d. For reoxidation experiments, the enzyme was first reduced with a 1.2-fold excess of substrate under anaerobic conditions. Different oxygen concentrations in the reoxidation mixture were obtained by equilibrating the buffer solutions with air (21% O_2), with commercially available N_2/O_2 mixtures (90 : 10, 50 : 50, v/v), or with pure O_2. Prior to experiments, oxygen was scrubbed from the stopped-flow apparatus with pure helium at 25 °C, and syringes were incubated with a dithionite solution for 16 h and then rinsed with deoxygenated buffer. In the reoxidation experiments, the final solution contained 100 mM glucose, 6 nM glucose oxidase, and 0.7 μM catalase.

To analyze the rate constants, traces of absorbance vs. time were extracted from the spectra vs. time data set. Traces from reductive half-reaction data at 455 nm were fit to a sum of exponentials equation to determine the rate constants using PROGRAM A (from D. P. Ballou, University of Michigan) and SPECFIT/32 software (Spectrum Software Associates). The same software was used to simulate the experimental traces, using a two-step kinetic model. Subsequently the rate constants were analyzed by least-means-squares curve fitting procedures with KALEIDAGRAPH (Synergy Software). Rate and dissociation constants were extracted according to the equations of Strickland *et al.* [12]. The diode-array data were deconvoluted using SPECFIT/32 software.

Enzyme-monitored turnover (EMTN) experiments were used to determine the steady state kinetic parameters of the reaction catalyzed by glycine oxidase. These measurements were performed with air-equilibrated (0.253 mM O_2) solutions at 25 °C according to Gibson *et al.* [13]. The area described by the experimental curve is proportional to the concentration of the limiting substrate (oxygen). During analysis, this area is divided into segments along the time axis. For each segment a velocity is calculated at the corresponding concentration of the remaining limiting substrate. Data traces at 455 nm were analyzed with KALEIDAGRAPH according to the method of Gibson *et al.* [13]. Oxygen was the limiting substrate. The concentration of the reducing substrate (at least five concentrations used) was varied over a range so as to obtain sufficient information about both K_m and k_{cat}.

Results

Steady state measurements

The catalytic mechanism of glycine oxidase with glycine, sarcosine, and D-proline as substrate was studied using the EMTN assay. In a previous study we identified the product composition of the reaction of glycine oxidase with glycine and sarcosine as substrate [4]. Both compounds yield glyoxylate and hydrogen peroxide but differ in the nitrogen containing product: ammonia or methylamine with glycine and sarcosine, respectively. The products of the oxidation reaction of D-proline were similarly analyzed. A Rank type oxygen electrode and an *o*-dianisidine/horseradish peroxidase coupled spectrophotometric assay indicated that hydrogen peroxide is the product of the oxygen reduction.

Neither the assay of α-keto acid by a reaction with 2,4-dinitrophenylhydrazine nor the glutamate dehydrogenase-coupled assay for ammonia detection revealed any spectral change [4]. These results suggest that the cyclic Δ^1-pyrrolidine-2-carboxylate is the product of D-proline oxidation by glycine oxidase, analogous to the reaction performed by D-amino acid oxidase on the same compound [14].

Glycine. The oxidized enzyme was mixed aerobically with glycine in the stopped-flow spectrophotometer and the change in flavin absorption monitored at 455 nm. A very rapid decrease in absorption was observed, amounting to 50% of the total change (Fig. 1). From this we deduced that the rate of enzyme reduction was similar or faster than the reoxidation rate under these conditions. The initial decrease of absorption was followed by a steady state phase, whose duration depended on initial glycine concentration and which led to the fully reduced enzyme as the final state. A steady state phase was observed only in a narrow range of substrate concentration. The 455 nm traces were analyzed as a function of oxygen concentration according to Gibson *et al.* [13]; the kinetic parameters obtained are given in Table 1.

The double-reciprocal plot in the inset of Fig. 1 shows a set of lines converging on the negative abscissa. This behavior is compatible with formation of a ternary complex mechanism (lower loop of Scheme 1) that, using the conventions of Dalziel [15], is described by the following steady state equation:

$$\frac{e_t}{v} = \phi_0 + \frac{\phi_S}{[Gly]} + \frac{\phi_{O_2}}{[O_2]} + \frac{\phi_{SO_2}}{[Gly][O_2]} \qquad (1)$$

where: $k_{cat} = 1/\phi_0, K_m^{Gly} = \phi_{Gly}/\phi_0, K_m^{O_2} = \phi_{O_2}/\phi_0$

The corresponding values of k_{cat}, K_m^{Gly} and $K_m^{O_2}$ are given in Table 1.

Sarcosine. The reaction of glycine oxidase with sarcosine was also studied by EMTN (Fig. 1). The results differed from those obtained with glycine because in the Lineweaver–Burk (inset of Fig. 1) the data can be satisfactorily fitted only using a set of parallel lines (and not a set of converging lines as for glycine). Such a pattern suggests that a ping-pong mechanism is active or that the ϕ_{SO_2} steady state coefficient is negligible at all sarcosine concentrations used. Interestingly, the values of the steady state kinetic parameters determined using sarcosine as substrate are quite close to those obtained using glycine (Table 1).

D-Proline. The reaction of glycine oxidase with the D-isomer of the cyclic amino acid proline was studied by the EMTN method as well using the stopped-flow spectrophotometer (Fig. 1). The initial decrease in absorbance at 455 nm following the aerobic mix of oxidized glycine oxidase with

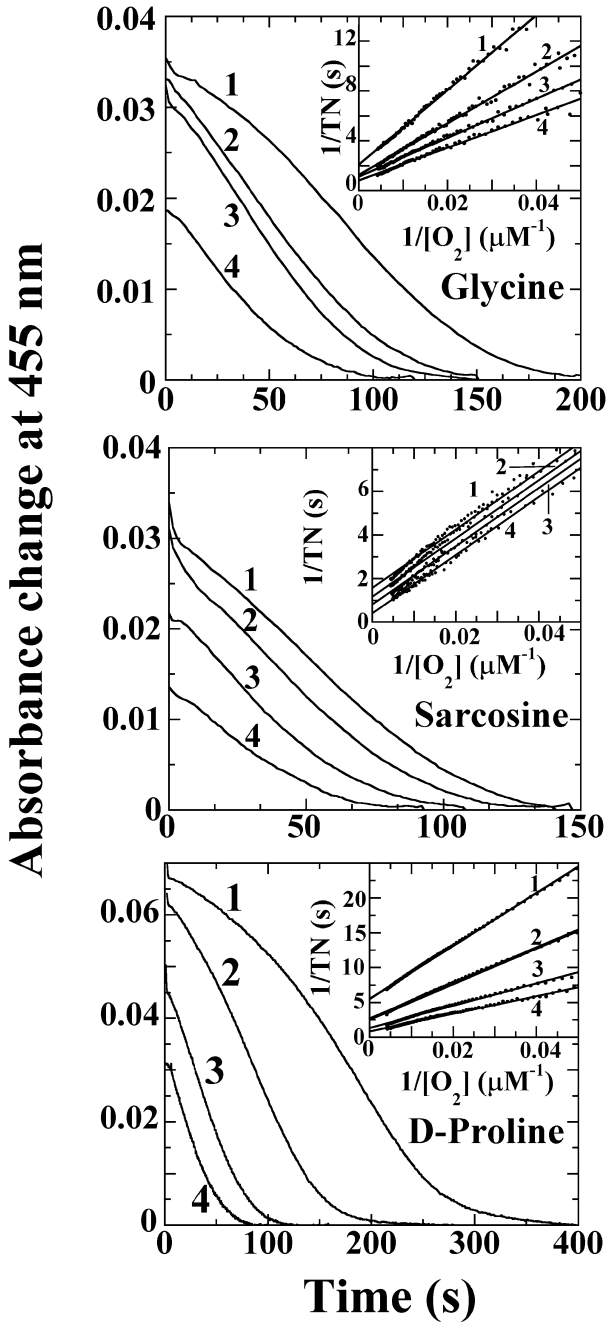

Fig. 1. Determination of turnover data for glycine oxidase with glycine, sarcosine, and D-proline in the presence of 0.253 mM oxygen using the stopped-flow instrument. Top panel: the enzyme (8 μM, $\Delta Abs_{tot} = 0.07$) was reacted with 0.7 mM (1), 1.0 mM (2), 1.6 mM (3), and 2.5 mM (4) glycine in 75 mM disodium pyrophosphate buffer, pH 8.5 at 0.253 mM O_2 (all final concentrations). The traces represent the course of the reaction, monitored at 455 nm. Middle panel: the enzyme (8 μM, $\Delta Abs_{tot} = 0.07$) was reacted with 0.7 mM (1), 1.25 mM (2), 1.6 mM (3), and 2.5 mM (4) sarcosine in 75 mM disodium pyrophosphate buffer, pH 8.5 at 0.253 mM O_2 (all final concentrations). The traces represent the course of the reaction, monitored at 455 nm. Bottom panel: The enzyme (10 μM, ΔAbs_{tot} approximately 0.09) was reacted with 5 mM (1), 10 mM (2), 25 mM (3), and 50 mM (4) D-proline in 75 mM disodium pyrophosphate buffer, pH 8.5 at 0.253 mM O_2 (all final concentrations). The traces represent the course of the reaction, monitored at 455 nm. Insets: Lineweaver–Burk representation of the same data as in the main graph, obtained as described by Gibson *et al.* [13].

Table 1. Specific steady state coefficients for the reaction of glycine oxidase with glycine, sarcosine and D-proline as substrate determined using the EMTN assay. Measurements were in 75 mM disodium pyrophosphate buffer, pH 8.5, at 25 °C. The steady state values are taken from slopes and intercepts as reported in Fig. 1 insets, according to the method of Dalziel [15]. The calculated K_m values obtained using the steady state equation for the sequential mechanism (Eqn 10 and Eqn 11) and the rate constants reported in Table 2 are reported in parentheses.

Substrate	Lineweaver–Burk pattern	$\Phi_0^{-1} = k_{cat}$ (s^{-1})	Φ_S (M·s) ($\times 10^{-3}$)	ϕ_{O_2} (M·s) ($\times 10^{-3}$)	ϕ_{SO_2} (M^2·s) ($\times 10^{-6}$)	K_m^S (mM)	$K_m^{O_2}$ (mM)
Glycine	≈ convergent	4.03 ± 1.08	0.96 ± 0.09	0.096 ± 0.014	0.138 ± 0.005	3.8 (2.0)	0.38 (0.48)
Sarcosine	parallel	4.15 ± 1.31	0.65 ± 0.1	0.102 ± 0.011	N.D.	2.6 (1.9)	0.42 (0.48)
D-Proline	≈ convergent	3.5 ± 1.75	22 ± 3.1	0.126 ± 0.021	1.48 ± 0.12	76.5 (81.6)	0.44 (0.35)

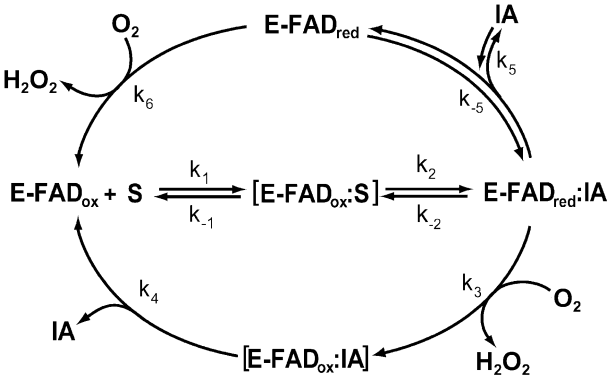

Scheme 1. Kinetic mechanisms for glycine oxidase. Intermediates not detected spectrophotometrically, but which were required by the kinetic mechanism, are shown in parentheses.

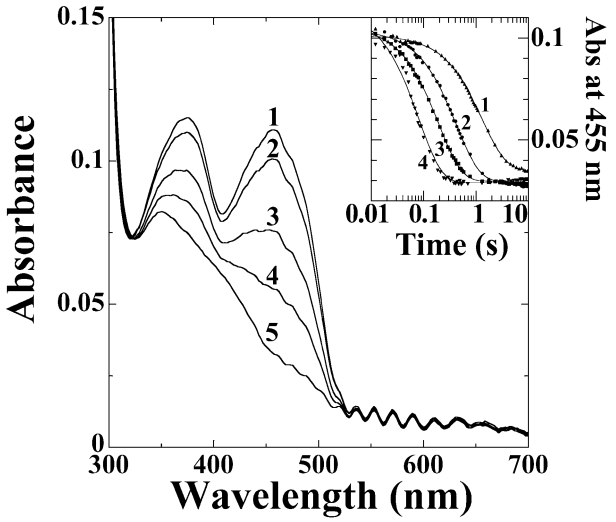

Fig. 2. Spectral courses of the anaerobic reduction of glycine oxidase by glycine followed in stopped-flow spectrophotometer. A total of 10 μM glycine oxidase in 75 mM disodium pyrophosphate buffer, pH 8.5, was mixed anaerobically with 2 mM glycine (final concentration). Spectra were recorded at 10 ms (1) (it corresponds essentially to the unreacted enzyme), 70 ms (2), 250 ms (3), 500 ms (4), and 1.5 s (5) after mixing. Inset: Course of anaerobic reduction of glycine oxidase followed in stopped-flow spectrophotometer. Time courses of reaction of 10 μM glycine oxidase (recorded at 455 nm) after mixing with 0.5 mM (1, ▲), 2 mM (2, ●), 5 mM (3, ■) and 15 mM (4, ▼) glycine (final concentrations). The points represent the experimental traces, and the continuous lines are the corresponding best fits obtained using a monoexponential algorithm.

the substrate was smaller than that observed with glycine and sarcosine and was approximately proportional to the concentration of D-proline. This observation indicates that the rate of flavin reduction is still quite close to that of reoxidation of the reduced enzyme form but slower than that determined with the other two substrates. As reported above using glycine as substrate, the Lineweaver–Burk plot (Fig. 1, inset) showed a set of convergent lines. The kinetic parameters are reported in Table 1 and show a significantly higher K_m value for the substrate D-proline (and Φ_S steady state parameter) than that determined for glycine and sarcosine, whereas the turnover number is similar to the ones determined with the two other substrates.

The reductive half-reaction

When the oxidized form of glycine oxidase was mixed anaerobically with glycine at 25 °C and pH 8.5, the yellow color bleached rapidly to yield the typical spectrum of the uncomplexed, reduced enzyme (Fig. 2) [4]. The time course was followed at 455 nm and was represented satisfactorily by a single exponential curve (inset of Fig. 2).

A plot of the observed reduction rates, k_{obs}, with increasing glycine and sarcosine concentration exhibited a slight curvature (Fig. 3A). The hyperbolic behavior on the direct plot has been analytically demonstrated by Strickland *et al.* [12] to describe a first-order reaction of a binary complex (k_2/k_{-2}) that follows a second-order complex formation (k_1/k_{-1}). This was interpreted as follows:

$$\text{E-FAD}_{ox} + \text{Gly} \underset{k_{-1}}{\overset{k_1}{\longleftrightarrow}} \text{E-FAD}_{ox}\text{:Gly} \underset{k_{-2}}{\overset{k_2}{\longleftrightarrow}} \text{E-FAD}_{red}\text{:iminoglyoxylate} \quad (2)$$

Steps k_1 and k_{-1} were not observed spectrophotometrically, implying that substrate binding did not affect the oxidized flavin chromophore to a measurable extent. The disappearance of absorption therefore reflects step k_2.

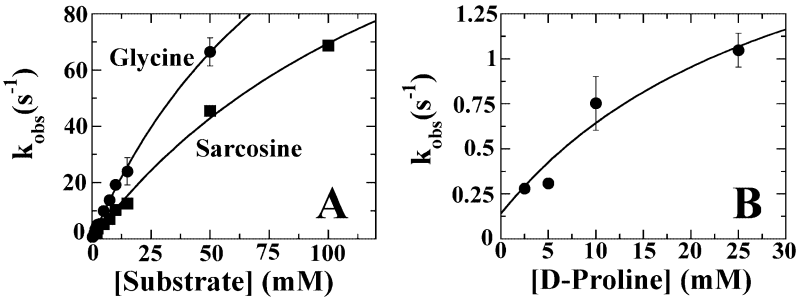

Fig. 3. Dependenceof the observed rate of anaerobic reduction of glycine oxidase on (A) glycine (●) and sarcosine (■) concentration, and (B) D-proline (●) concentration. (A) Conditions as those reported in Fig. 2. Vertical bars indicate ± SE for five determinations. When not shown, the standard error is smaller then the symbols used.

According to Strickland *et al.* [12], the linearity of the double-reciprocal plots of k_{obs} vs. [S] (data not shown) is compatible with a situation in which $k_{-2} \ll k_2$ and $k_{-2} \approx 0$, i.e. an almost irreversible reduction step preceded by the attainment of rapid equilibrium between free enzyme and substrate-bound enzyme, i.e. $k_{-1} > k_2$ (Eqn 2). By simulating the experimental traces with Specfit/32 software, the absorbance changes could be reasonably duplicated using the absorbance spectrum of free-oxidized and fully reduced glycine oxidase [4] and showed minimal values for k_1 of 20000 $M^{-1}{\cdot}s^{-1}$ and for k_{-1} of 1200 s^{-1} for glycine oxidase with glycine and sarcosine as substrate (Table 2).

Using D-proline as substrate, however, two main differences are evident as compared to glycine and sarcosine: the rates of flavin reduction are lower at all substrate concentrations used and the primary plot of k_{obs} vs. [substrate] showed a clear *y*-intercept (Fig. 3B), pointing to a reversible rate of flavin reduction k_{-2} different from zero [12]. This is particularly evident in the corresponding double-reciprocal plot that shows a plateau at high 1/[S] (data not shown). From such a plot, a k_{-2} value of ≈ 0.2 s^{-1} was estimated.

The extrapolated rates of reduction of glycine oxidase for the substrates tested are reported in Table 2 and show similar reduction rates for glycine and sarcosine. In contrast, using D-proline as substrate, the rate of flavin reduction was significantly lower and the $K_{d,app}$ (corresponding to the ratio of slope to intercept of the double-reciprocal plot of k_{obs} vs. substrate concentration) was significantly higher than the corresponding values determined for the other substrates. The estimated value of $K_{d,app}$ for D-proline (640 mM) is four- to eightfold greater than the value determined for glycine and sarcosine. Simulation of the spectral courses during glycine oxidase reduction by D-proline using SPECFIT/32 indicated that the increase in $K_{d,app}$ value is due to an increase in the rate constant for substrate dissociation from the oxidized form (k_{-1} rate constant in Eqn 2).

A feature of many flavin-dependent oxidases is that they form relatively stable reduced enzyme-product complexes, which often have characteristic charge transfer absorptions and can be detected spectrophotometrically [16]. For this reason, formation of the fully reduced uncomplexed species is often observed to follow a biphasic course [17–19]. By contrast, the reduction course of glycine oxidase was essentially monophasic, indicating that the reduced enzyme:iminoacid (IA) complex or its dissociation are not detectable spectroscopically (step k_5 in Scheme 1). A similar situation was observed for the reaction of cholesterol oxidase with cholesterol as substrate [20]. Therefore, we attempted to detect spectral changes during anaerobic titrations of glycine oxidase with iminoglyoxylate by differential spectroscopy. As this compound is unstable in aqueous solution (it is in equilibrium with glyoxylate and ammonia), we tried to produce it by adding glyoxylate and ammonium chloride to the enzyme solution (analogously to that previously performed for D-amino acid oxidase and iminopyruvate) [19]. The result of anaerobic titration of fully reduced glycine oxidase (obtained by anaerobic reaction with a twofold excess of glycine) using increasing concentrations of glyoxylate in the presence of 400 mM ammonium chloride was the production of the oxidized enzyme form (Fig. 4). From the changes in absorbance at 455 nm an apparent K_d value of 21.6 ± 3.8 mM was determined for the overall equilibrium reported in Eqn (2) and Eqn (3).

$$\text{E-FAD}_{red}\text{:iminogyloxylate} \longleftrightarrow \text{E-FAD}_{red} + \text{iminogyloxylate}$$

$$\text{iminoglyoxylate} + H_2O \longleftrightarrow NH_4^+ + \text{glyoxylate} \quad (3)$$

In order to shift the equilibrium towards the E-FAD_{red}:IA complex, the anaerobic titration by glyoxylate was analogously performed using a large excess of glycine to reduce the

Table 2. Specific rate constants obtained for reductive half-reaction of glycine oxidase with glycine, sarcosine and D-proline as substrate in stopped-flow experiments. Measurements were in 75 mM disodium pyrophosphate buffer, pH 8.5, at 25 °C. The k_1 and k_{-1} rate constants are the minimal values determined by computer simulation of the experimental traces using SPECFIT/32, the k_2 rate constants reported in parenthesis, the absorbance spectrum of oxidized and fully reduced glycine oxidase [4] and Eqn (2).

	k_{red} (k_2) (s^{-1})	k_{-2} (s^{-1})	$K_{d,app}$ ($\approx k_{-1}/k_1$) (mM)	k_1 ($M^{-1}{\cdot}s^{-1}$)	k_{-1} (s^{-1})	1/Slope ($\approx k_2{\cdot}k_1/k_{-1}$) ($M^{-1}{\cdot}s^{-1}$) ($\times 10^3$)
Glycine	166 ± 16.4 (150)	–	142 ± 21.1	20000	1200	1.17
Sarcosine	170 ± 33.1 (150)	–	84 ± 4.0	20000	1200	2.10
D-Proline	26 ± 7.5 (30)	0.20 ± 0.06	640 ± 120	40000	20000	0.041

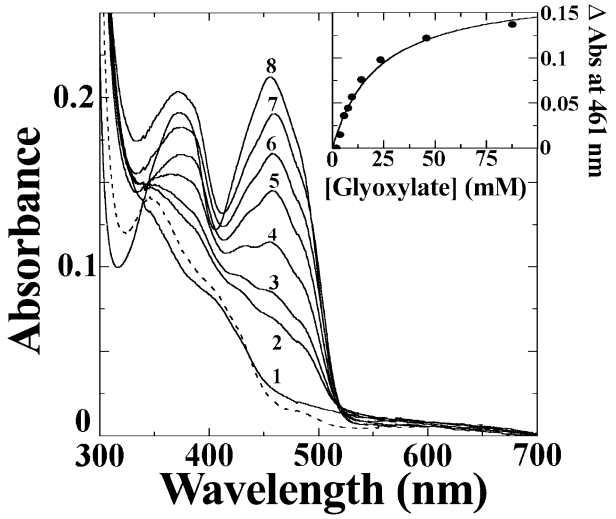

Fig. 4. Static titration of reduced glycine oxidase with glyoxylate in the presence of ammonia and under anaerobic conditions. A total of 18 μM reduced glycine oxidase (obtained by anaerobic reduction with a twofold excess of glycine) in 75 mM disodium pyrophosphate buffer, pH 8.5, containing 400 mM ammonium chloride (1) was added to (2) 1.9 mM (3) 3.8 mM (4) 7.6 mM (5) 19 mM (6) 37.5 mM (7) 82.6 mM, and (8) 167 mM glyoxylate. The dotted line shows the spectrum of a similar amount of reduced glycine oxidase after addition of 92 mM glycine, 400 mM ammonium chloride, and 44 mM glyoxylate. Inset: Effect of glyoxylate concentration of the absorbance at 461 nm during the titration.

enzyme (92 mM glycine). Up to 50 mM glyoxylate the spectrum of the reduced enzyme was unchanged, whereas the spectrum of the oxidized enzyme form appeared at the highest keto acid concentration (the spectrum of the reduced enzyme after the addition of 400 mM ammonium chloride and 44 mM glyoxylate is presented in Fig. 4 in comparison to the fully reduced one). A similar titration was also performed on the reduced glycine oxidase by adding a threefold excess of sarcosine and 400 mM ethylamine and increasing the amount of glyoxylate (the products of the glycine oxidase reaction on sarcosine as substrate): during the titration the oxidized spectrum of the enzyme appeared (an apparent $K_d \approx 4$ mM has been estimated). A further confirmation that iminoglyoxylate converts the reduced enzyme form of glycine oxidase to the corresponding oxidized one was achieved by analyzing the effect of adding glyoxylate and glyoxylate plus ammonia separately. In fact, the anaerobic addition of 100 mM glyoxylate to the reduced form of glycine oxidase did not result in significant changes in the absorbance spectrum of the reduced enzyme, whereas, upon the addition of 400 mM ammonium chloride, the corresponding oxidized form appeared (it is not attributable to oxygen leak, as the subsequent addition of 15 mM glycine did not restore the absorbance spectrum corresponding to the reduced enzyme). These results demonstrate that the reductive half-reaction is reversible: hence, although the value of k_{-2} in Eqn (2) is very small, it is different from zero with all the substrates used. The spectral traces reported in Fig. 4 at varied concentrations of glyoxylate were simulated using SPECFIT/32 software, the k_2, k_{-2} and K_d values for glycine binding to the oxidized enzyme determined from the forward reaction (Table 2) and the extinction coefficients of free oxidized and free reduced glycine oxidase [4]. Simulations yielded the rate constants $k_5 \approx 1$ s^{-1} and $k_{-5} \approx 15$–100 M^{-1}·s^{-1}. These estimated values clearly show that the release of the imino acid from the reduced glycine oxidase is slow in comparison to the rate of flavin reduction and to the turnover number (Tables 1 and 2).

The oxidative half-reaction

The reduced glycine oxidase was prepared by adding a 1.2-fold excess of glycine under anaerobic conditions. The uncomplexed, reduced form of glycine oxidase was reacted in the stopped-flow instrument with buffer containing various oxygen concentrations, and spectra were recorded during reoxidation (Fig. 5). The experimental absorbance traces at 455 nm closely fit a single exponential rate process, i.e. they were essentially monophasic. The reoxidation rates depended linearly on the oxygen concentration (no indication of saturation with O_2 was seen) and could be extrapolated to the origin – consistent with a second-order reaction in dioxygen (Fig. 6).

$$\text{E-FAD}_{red} + O_2 \xrightarrow{k_6} \text{E-FAD}_{ox} \sim H_2O_2 \longleftrightarrow \text{E-FAD}_{ox} + H_2O_2 \quad (4)$$

However, there is no measurable spectral change associated with H_2O_2 release, and it is thus not observed.

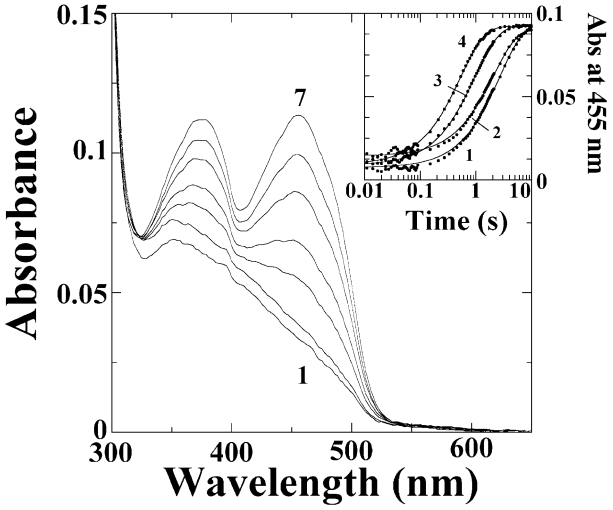

Fig. 5. Course of reoxidation of free reduced glycine oxidase followed in stopped-flow spectrophotometer. Main figure: Spectral course of reoxidation after mixing 10.5 μM reduced glycine oxidase with a buffer saturated with 30.25% (0.365 mM) oxygen. Spectra (from bottom to top) were recorded 10 ms (1), 100 ms (2), 300 ms (3), 500 ms (4), 900 ms (5) 1.5 s (6), and 8.1 s (7) after mixing. Conditions: 75 mM disodium pyrophosphate buffer, pH 8.5, containing 100 mM glucose, 6 nM glucose oxidase, and 0.7 μM catalase, at 25 °C. The reduced form of glycine oxidase was obtained by anaerobic incubation with 1.2-fold excess of glycine. Inset: Time courses (recorded at 455 nm) of reaction of reduced glycine oxidase with buffer saturated with 5% (1), 10.5% (2), 25% (3) and 50% (4) oxygen (final concentrations). The points represent the experimental traces, and the continuous lines are corresponding best fits obtained using a monoexponential algorithm.

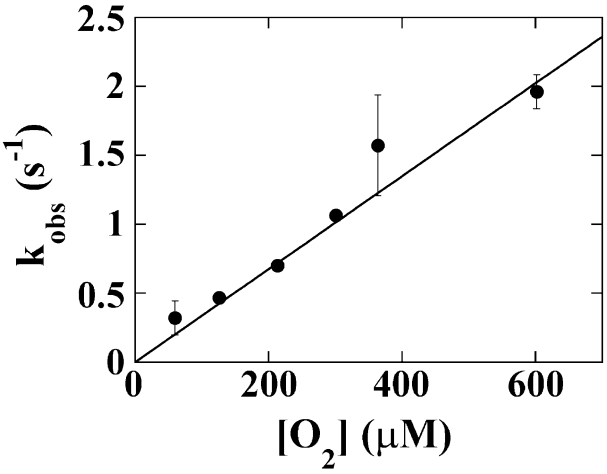

Fig. 6. Dependence of the observed rate of reoxidation of reduced glycine oxidase on oxygen concentration. Reoxidation rates obtained by mixing the reduced enzyme solutions equilibrated with different concentration of oxygen as detailed in Fig. 5. The data points are the average of five single measurements determined using the stopped-flow instrument following the absorbance increase at 455 nm. When not shown, the standard error bars were smaller than the symbols used.

The observed rate of reoxidation ($k_6 = 3.3 \times 10^3$ M^{-1}·s^{-1}) is lower than the $1/\phi_{O_2}$ steady state parameter and thus too slow to be significant in turnover (Table 1). It is therefore likely that the reoxidation involves reduced enzyme bound to the intermediate imino acid product, according to Eqn (5).

$$\text{E-FAD}_{red}\text{:IA} + O_2 \xrightarrow{k_3} \text{E-FAD}_{ox}\text{:IA} + H_2O_2 \underset{k_{-4}}{\overset{k_4}{\longleftrightarrow}} \text{E-FAD}_{ox} + \text{IA} \quad (5)$$

In general, it is difficult to prepare the E-FAD$_{red}$:IA complex due to the spontaneous solvolysis of the imino acids to ammonia and α-keto acids. The K_d constant estimated for binding of the IA to reduced yeast and mammalian D-amino acid oxidases, as determined by anaerobic titration, was 2–4 mM [19,21,22]. In the case of glycine oxidase, complexes are formed which cannot be detected spectrophotometrically (i.e. they possess very low extinction) and the overall equilibrium is fully reversible (Fig. 4). Thus, an IA concentration could not be identified that was sufficient to ensure essentially complete E-FAD$_{red}$:IA complex formation for use in the oxidation experiments referred to above. Thus, in order to study the oxidation of the reduced, binary complex, the oxidative half-reaction was performed by mixing the anaerobic reduced enzyme with O_2-saturated buffer solutions containing 100 mM glyoxylate and 400 mM ammonia. The 455 nm-absorbance traces of flavin reoxidation, as well as the observed reaction rates, were similar to those determined in the absence of ammonia and glyoxylate. This suggests that the reoxidation still results from the free reduced enzyme form, i.e. the rate of flavin reoxidation is faster than the formation of the reduced enzyme-iminoglyoxylate complex.

As stated above, the absorbance increase at 455 nm during the reoxidation experiments follows a first-order process, i.e. the release of IA from the reoxidized enzyme:IA complex is not detectable spectrophotometrically. The binding of iminoglyoxylate to the oxidized form of glycine oxidase was investigated by static titration using increasing amounts of glyoxylate in the presence of 400 mM ammonia (to shift the equilibrium toward IA production). The addition of glyoxylate up to 260 mM only resulted in small spectral changes ($\Delta\varepsilon \leq 1000$ M^{-1}·cm^{-1}) at wavelengths ≥400 nm, confirming the results from rapid kinetic studies. On the other hand, at lower wavelengths a more intense hyperchromic shift was observed, thus allowing the calculation of an estimated apparent $K_d \approx 10$ mM for the binding of iminoglyoxylate to the oxidized form of glycine oxidase (data not shown). Interestingly, and analogously to that observed for the binding to the reduced form of glycine oxidase, a similar spectral change was not detected during the titration of the enzyme with glyoxylate in the absence of ammonia, thus demonstrating that it is specifically due to the binding of the IA.

Discussion

Our previous findings on substrate specificity of glycine oxidase [3,4] indicated that it partially overlaps with that of D-amino acid oxidase and SOX. Therefore, the kinetic mechanism of glycine oxidase was studied in detail using three different compounds that are among the best substrates of this new flavooxidase. Sarcosine was used because it is the substrate of SOX and glycine because it is oxidized (although with a low efficiency) by D-amino acid oxidase. D-Proline was instead used because it is the only D-amino acid which is oxidized by both D-amino acid oxidase and D-aspartate oxidase [5] and because monomeric SOX was demonstrated to oxidize its L-isomer [23].

The reductive half-reaction

The converging lines for glycine oxidase in Lineweaver–Burk plots using glycine and D-proline as substrate (Fig. 1 inset) indicate a ternary complex mechanism. By contrast, double-reciprocal plots were quite parallel using sarcosine. Parallel plots are to be expected as the reductive half-reaction is almost irreversible ($k_2 \gg k_{-2}$) (Eqn 2). The validity of such a conclusion is supported by the results of primary trace simulations, where superimposing the experimental and calculated traces requires that $k_2 \gg k_{-2}$ (not shown). Such a conclusion was experimentally demonstrated in the case of D-proline as substrate: because the value of k_2 is small, the reversal rate $k_{-2} \approx 0.2$ s^{-1} has been directly estimated (Fig. 3B). Static titration of the reduced enzyme:imino acid complex with increasing amounts of glyoxylate in the presence of 400 mM ammonia yielded the spectrum of the oxidized enzyme form (Fig. 4), thus confirming that the reductive half-reaction is reversible under appropriate experimental conditions, i.e. that k_{-2} is low but different from zero. A similar situation was also reported for the reductive half-reaction of G99S mutant of lactate monooxygenase [24]. Simulation of the static titration of reduced glycine oxidase by glyoxylate in the presence of 400 mM ammonia made it possible to estimate the rate constant of IA release from E-FAD$_{red}$ (k_5 in Scheme 1), thus showing that it is significantly lower than k_2 and k_{cat}

values. Using similar simulations the lowest limits for k_1 and k_{-1} as listed in Table 2 could also be estimated.

For all substrates, the enzyme-substrate complex was essentially in equilibrium with the enzyme plus substrate, i.e. $k_{-1} \gg k_2$ (Eqn 2). Based on this situation, the ordinate intercept of the double-reciprocal plot of the reduction rates yields $1/k_2$ and the slope corresponds to $k_{-1}/(k_1 \cdot k_2)$ [12]. In such a case, the ratio of slope to intercept yields the true $K_d = k_{-1}/k_1$ [12]. The K_d values reported in Table 2 agree nicely with the theoretical values obtained using the estimated k_1 and k_{-1} values, confirming the validity of the reported rate constants.

It is important to note that the rates of reduction using glycine, sarcosine, and D-proline were significantly higher than the k_{cat} values for the enzyme under the same experimental conditions (Tables 1 and 2), thus demonstrating that the rate-limiting step belongs to the oxidative half-reaction.

The oxidative half-reaction

A major finding of this study is that the apparent rate of reoxidation of the free reduced glycine oxidase was not consistent with the turnover rate and steady state coefficients. The plot of the observed rates of reoxidation as the function of oxygen concentration yielded a straight line passing through the origin (Fig. 6). In general, such behavior is taken to indicate a second-order reaction of the reduced enzyme with O_2 without the presence of definite intermediates. In fact, absorption spectra recorded during reoxidation provide no indication of such an intermediate (Fig. 5). The threefold discrepancy between the rate of E-FAD$_{red}$ reoxidation (the slope of the plot in Fig. 6, $k_6 = 3.3 \times 10^3$ M^{-1}·s^{-1}) and the steady state parameter $1/\phi_{O_2}$ determined under the same experimental conditions (1×10^4 M^{-1}·s^{-1}) points to a mechanism by which oxygen reacts with the reduced enzyme prior to the release of the first product. Because of the impossibility of quantitatively producing the E-FAD$_{red}$:IA complex, the oxygen reactivity of such an enzyme form was not solved.

The overall mechanism

The cycle catalyzed by glycine oxidase is consistent with the kinetic mechanism reported in the lower loop of Scheme 1, which is analogous to that proposed for D-amino acid oxidase [18,19,22]. The finding of a parallel line pattern in the Lineweaver–Burk plots obtained with sarcosine as substrate and of a converging line pattern with glycine and D-proline as substrate indicates a limiting case of a ternary complex mechanism, where some specific rate constants are sufficiently small. A similar situation was observed with D-amino acid oxidase [18,19]: the reductive half-reaction was considered practically irreversible because $k_2 \gg k_{-2}$.

As noted previously, the data for glycine oxidase indicate a ternary complex mechanism.

$$\phi_0 = (k_4 + k_2)/k_2 \cdot k_4 \approx 1/k_4 \text{ (if } k_2 \gg k_4) \quad (6)$$

$$\phi_S = (k_{-1} + k_2)k_1 \cdot k_2 \quad (7)$$

$$\phi_{O_2} = (k_2 + k_{-2})/k_2 \cdot k_3 \approx 1/k_3 \quad (8)$$

$$\phi_{O_2} = (k_{-1} + k_{-2})/k_1 \cdot k_2 \cdot k_3 \approx \text{zero} \quad (9)$$

For all the substrates used, the reductive half-reaction is not rate limiting, as suggested by k_2 values (the rate of flavin reduction) that are higher than the k_{cat} values. This suggests that the rate of product dissociation from the complex with the enzyme in oxidized form (k_4 of Scheme 1) is slow and does affect the turnover number ($\Phi_0 \approx 1/k_4$). By using the measured values of k_{cat} and k_2, a lower limit for k_4 of 4.8 s^{-1} can be estimated (Eqn 6). Equation 8 defines the steady state parameter $1/\phi_{O_2} = k_2 \cdot k_3/(k_2 + k_{-2})$. For a reaction such as that studied here, $k_{-2} \ll k_2$ and $1/\phi_{O_2}$ reduces to k_3. The steady state coefficient $1/\phi_{O_2}$ is threefold greater than k_6 (the appropriate value of $1/\phi_{O_2}$ for the case of a ping-pong mechanism). Interestingly, an approximately threefold difference in oxygen reactivity between free reduced and E-FAD$_{red}$:IA complex has been also reported for D-amino acid oxidase [18,19]. The validity of this model is also supported by the reasonable agreement between the K_m values measured for the substrate and for O_2 and the calculated values (Table 1).

$$K_S = \phi_S/\phi_0 = k_4(k_{-1} + k_2)/(k_1 \cdot k_{-2}) \quad (10)$$

$$K_{O_2} = \phi_{O_2}/\phi_0 = k_4/k_3 \quad (11)$$

Conclusions

The kinetic mechanism of glycine oxidase resembles that recently determined for monomeric SOX on L-proline as substrate [23] and that of D-amino acid oxidase with neutral substrates [18,19]. In all these cases, the reaction follows a sequential mechanism in which the reoxidation starts from the E-FAD$_{red}$:IA complex. A main difference can be found in the rate-limiting step of catalysis: it has been demonstrated to be product dissociation in glycine oxidase and in mammalian D-amino acid oxidase [18] and the rate of flavin reduction in monomeric SOX [23] and yeast D-amino acid oxidase [19]. The crystal structure of D-amino acid oxidase from pig kidney [8] showed that the rate-limiting step is due to the movement of a long loop (amino acids 216–228) covering the active site and controlling the rate of product release. Such a 'slow' conformational change was partially overcame in yeast D-amino acid oxidase, where the loop was replaced by a single side chain (Tyr238) that swings between an opened and a closed form [25,26]. For such a structural reason, in yeast D-amino acid oxidase the rate-limiting step does not belong to the oxidative half-reaction but rather it is represented by the chemical step of flavin reduction (k_2 in Scheme 1) and thus its catalytic efficiency is significantly higher ($k_{cat} = 300$ s^{-1} at pH 8.3 and 25 °C) [19]. The turnover numbers determined for glycine oxidase are close to those for mammalian D-amino acid oxidase and D-alanine as substrate (approximately 10 s^{-1} at pH 8.3 and 25 °C) [18] and significantly lower than those determined for MSOX and sarcosine (k_{cat} approximately 117 s^{-1}, at pH 8.0 and 25 °C) [23]. The low catalytic efficiency of glycine oxidase does not clarify if glycine and/or sarcosine are the real substrates of this new flavoenzyme (this point will need of further investigations). A further feature distinguishing glycine oxidase from MSOX is that for the latter enzyme, L-proline is a slow substrate: k_{cat} (0.4 s^{-1}) is only 1% of the

rate observed with sarcosine. In contrast, for glycine oxidase all the substrates tested were oxidized at similar turnover rates (k_{cat} approximately 4 s^{-1}, Table 1). Concerning the reversibility of the reductive half-reaction, glycine oxidase is profoundly different from both D-amino acid oxidase and MSOX.

In conclusion, the investigation of the kinetic mechanism shows that glycine oxidase from *B. subtilis* resembles mammalian D-amino acid oxidase and can be distinguished from MSOX by the lower catalytic efficiency that results from a much lower rate of product dissociation from E-FAD_{ox}:IA complex. This suggests that different structural devices to control catalysis and different substrate specificity have evolved in glycine oxidase and MSOX. The results of this study and knowledge of the 3D structure of glycine oxidase are prerequisites for comparing the structure-function relationships in enzymes catalyzing similar reactions and possessing different substrate specificities, thus contributing to the clarification of the mechanism of oxidation of amine substrates by flavooxidases.

Acknowledgements

This work was supported by grants from Ministero dell'Istruzione, dell'Università e della Ricerca (Fondo di Ateneo per la Ricerca 2000) to Loredano Pollegioni.

References

1. Kunst, F., Ogasawara, N., Moszer, I., Albertini, A.M., Alloni, G., Azevedo, V., Bertero, M.G. *et al.* (1997) The complete genome sequence of the Gram-positive bacterium *Bacillus subtilis*. *Nature* **390**, 249–256.
2. Nishiya, Y. & Imanaka, T. (1998) Purification and characterization of a novel glycine oxidase from *Bacillus subtilis*. *FEBS Lett.* **438**, 263–266.
3. Job, V., Molla, G., Pilone, S.M. & Pollegioni, L. (2002) Overexpression of a recombinant wild-type and His-tagged *Bacillus subtilis* glycine oxidase in *Escherichia coli*. *Eur. J. Biochem.* **269**, 1456–1463.
4. Job, V., Marcone, G.L., Pilone, S.M. & Pollegioni, L. (2002) Glycine oxidase from *Bacillus subtilis*. Characterization of a new flavoprotein. *J. Biol. Chem.* **277**, 6985–6993.
5. Curti, B., Ronchi, S. & Pilone, S.M. (1992) D- and L-amino acid oxidases. In *Chemistry and Biochemistry of Flavoenzymes* (Müller, F., ed.), pp. 69–94. CRC Press, Boca Raton.
6. Pilone, S.M. (2000) D-amino acid oxidase: new findings. *Cell Mol. Life Sci.* **57**, 1732–1747.
7. Wagner, M.A. & Schuman Jorns, M. (1997) Folate utilization by monomeric versus heterotetrameric sarcosine oxidases. *Arch. Biochem. Biophys.* **342**, 176–181.
8. Mattevi, A., Vanoni, M.A., Todone, F., Rizzi, M., Teplyakov, A., Coda, A., Bolognesi, M. & Curti, B. (1996) Crystal structure of D-amino acid oxidase: a case of active site mirror-image convergent evolution with flavocytochrome b_2. *Proc. Natl Acad. Sci. USA* **93**, 7496–7501.
9. Trickey, P., Wagner, M.A., Schuman Jorns, M. & Mathews, F.S. (1999) Monomeric sarcosine oxidase: structure of a covalently flavinylated amine oxidizing enzyme. *Structure* **7**, 331–345.
10. Umhau, S., Pollegioni, L., Molla, G., Diederichs, K., Welte, W., Pilone, S.M. & Ghisla, S. (2000) The X-ray structure of D-amino acid oxidase at very high resolution identifies the chemical mechanism of flavin-dependent substrate dehydrogenation. *Proc. Natl Acad. Sci. USA* **97**, 12463–12468.
11. Harris, C.M., Pollegioni, L. & Ghisla, S. (2001) pH and kinetic isotope effects in D-amino acid oxidase catalysis. Evidence for a concerted mechanism in substrate dehydrogenation via hydride transfer. *Eur. J. Biochem.* **268**, 5504–5520.
12. Strickland, S., Palmer, G. & Massey, V. (1975) Determination of dissociation constants and specific rate constants of enzyme-substrate (or protein–ligand) interactions from rapid reaction kinetic data. *J. Biol. Chem.* **250**, 4048–4052.
13. Gibson, Q.H., Swoboda, B.E.P. & Massey, V. (1964) Kinetics and mechanism of action of glucose oxidase. *J. Biol. Chem.* **259**, 3927–3934.
14. Yagi, K., Nishikimi, M., Ohishi, N. & Takai, A. (1970) Release of alpha imino acid as primary product in D-amino-acid oxidase reaction. *Biochim. Biophys. Acta* **212**, 243–247.
15. Dalziel, K. (1969) The interpretation of kinetic data for enzyme-catalysed reactions involving three substrates. *Biochem. J.* **114**, 547–556.
16. Ghisla, S. & Massey, V. (1991) L-Lactate oxidase. In *Chemistry and Biochemistry of Flavoenzymes*, Vol. II (Müller, F., ed.), pp. 243–289. CRC Press, Boca Raton.
17. Lockridge, O., Massey, V. & Sullivan, P.A. (1972) Mechanism of action of the flavoenzyme lactate oxidase. *J. Biol. Chem.* **247**, 8097–8106.
18. Porter, D.J.T., Voet, J.G. & Bright, H.J. (1977) Mechanistic features of the D-amino acid oxidase reaction studied by double stopped flow spectrophotometry. *J. Biol. Chem.* **252**, 4464–4473.
19. Pollegioni, L., Langkau, B., Tischer, W., Ghisla, S. & Pilone, S.M. (1993) Kinetic mechanism of D-amino acid oxidase from *Rhodotorula gracilis* and *Trigonopsis variabilis*. *J. Biol. Chem.* **268**, 13850–13857.
20. Pollegioni, L., Wels, G., Pilone, S.M. & Ghisla, S. (1999) Kinetic mechanism of cholesterol oxidase from *Streptomyces hygroscopicus* and *Brevibacterium sterolicum*. *Eur. J. Biochem.* **264**, 140–151.
21. Massey, V. & Gibson, Q.H. (1964) Role of the semiquinones in flavoprotein catalysis. *Fed. Proc. Fed. Am. Soc. Exp. Biol.* **23**, 18–29.
22. Fitzpatrick, P.F. & Massey, V. (1982) Proton release during the reductive half- reaction of D-amino acid oxidase. *J. Biol. Chem.* **257**, 9958–9962.
23. Wagner, M.A. & Schuman Jorns, M. (2000) Monomeric sarcosine oxidase: 2. Kinetic studies with sarcosine, alternate substrates, and substrate analogue. *Biochemistry* **39**, 8825–8829.
24. Sun, W., Williams, C.H. Jr & Massey, V. (1997) The role of the glycine 99 in l-lactate monooxygenase from *Mycobacterium smegmatis*. *J. Biol. Chem.* **272**, 27065–27076.
25. Boselli, A., Sacchi, S., Job, V., Pilone, S.M. & Pollegioni, L. (2002) Role of tyrosine 238 in the active site of *Rhodotorula gracilis* D-amino acid oxidase. A site directed mutagenesis study. *Eur. J. Biochem.* **269**, 4762–4771.
26. Pollegioni, L., Diederichs, K., Molla, G., Umhau, S., Welte, W., Ghisla, S. & Pilone, S.M. (2002) Yeast D-amino acid oxidase: structural basis of its catalytic properties. *J. Mol. Biol.* **324**, 535–546.